
THE 18TH INTERNATIONAL ELECTRIC VEHICLE SYMPOSIUM
EXIT
THE WORLD'S LARGEST EVENT FOR ELECTRIC VEHICLES
THE PAPERS
EXHIBITORS
SPONSORS
INFO
The 18th International Electric Vehicle Symposium and Exhibition
October 20 - 24, 2001
Berlin, Germany
EVS 18

A Dynamical Model of Proton Exchange Membrane Fuel Cell

M. Ceraolo, R. Giglioli, C. Miulli, A. Pozio

Abstract

The article presents a simplified dynamical model of a fuel cell of the Proton Exchange Membrane (PEM) type, based on physical-chemical knowledge of the phenomena occurring inside the cell.
Since the anodic overvoltages influence the cell behaviour to a lower extent than cathodic and ohmic overvoltages, they have been disregarded for simplicity.
The model needs several parameters to be identified; however, it has been built so that all of them can be identified by means of simple measures on cells on steady-state and dynamic conditions.

The model has been implemented in the MATLAB/SIMULINK environment.
Lab tests have been carried out at ENEA's laboratories; the paper presents a good agreement between tests and simulations, both in static and dynamic conditions.

Keywords: fuel cell, modeling, simulation.

1. Introduction

The need of reducing pollutant emissions and of utilising more efficiently the available energy resources (in particular fossil resources) has caused, in recent years, an ever increasing attention towards fuel cells. In fact, their high conversion efficiency and low environmental impact, make them good candidates for substituting, at least in some applications, more conventional conversion systems.

One of the applications of Fuel Cells currently being considered is as a source of energy for electric vehicles, normally in hybrid configuration.
Among the several possible kinds of fuel cells, the Polimer Electrolyte Fuel Cells (PEFC), also called Proton Exchange Membrane Fuel Cells (PEM), appear to be the best candidate for the use aboard of Electric Vehicles in which simplicity, high specific power, rapid start-up (even at low temperature) have the maximum importance [4, 11, 16].

To be able to utilise these devices in an effective way, it is, however, mathematical models of the vehicle fuel cell stack are necessary so that the system behaviour can be analysed at the design stage by means of computer simulations in different conditions of load, pressure of reagent gases, temperature.
These models can be integrated with other components in vehicle simulation environments (such as the one described in [17]), so that the whole system of a fuel cell vehicle can be analysed in detail.

Several mathematical model of PEM fuel cells have already been presented [4÷12]. The majority of them, however, is able to simulate only the cell steady-state behaviour, while the analysis of their performance in dynamic conditions is important for the use aboard of vehicles, given the rapid variation of mechanical and electrical quantities.
Other models [7, 11] are characterised by a high complexity, with several partial-derivatives equations to be kept into account. This high complexity creates problems of simulation times, parameter identifications, etc. especially when they are to be enclosed into a larger system, such as the electric vehicle.

The purpose of this paper, therefore, is to propose a dynamical model of PEM fuel cells that, although simplified, is still based on the knowledge of the chemical-physical description of the phenomena occurring inside the cell.

The effort carried-out was to simplify as much as possible the analytical aspects, so that simulation and numerical parameter identification are eased.
The model is implemented in the well known and highly widespread simulation environment MATLAB/SIMULINK.

2. Mathematical model

2.1. A simple description of the cell structure

A PEM Fuel Cell is constituted by a membrane able to conduct protons disposed between two electrodes. The set electrodes-membrane, in turn, is pressed by two conductive plates containing some channels in which the reactants flow.
A simplified representation of the cell is reported in fig. 1. The main elements composing the cell are: conductor plates, electrodes, membrane.
The electrodes are constituted by a **gas diffusion baking**, made of carbon (graphitic) paper or cloth, and a **catalyst layer**; both have a porous, partially hydrophobic, structure.
According to several studies [3÷11], the larger pores (called ***macropores***) operate as a ducts for the reactants from the flow channels towards the catalyst layer, while the smaller ones (***micropores***) operate as a ducts for the passage of water.

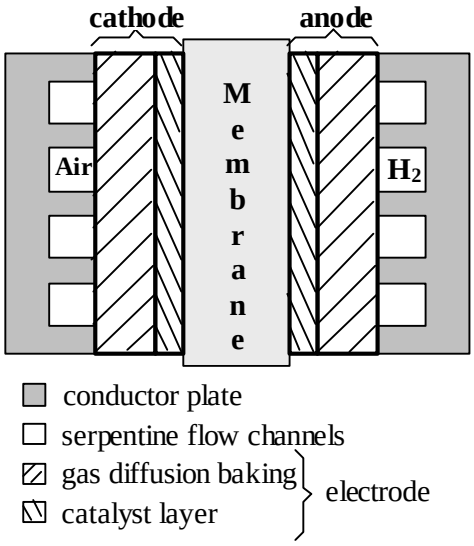

Figure 1: Schematic representation of fuel-cell of PEM type.

The reactions occurring in the catalytic layer of the electrodes are the following ones:

- at the anode the hydrogen decomposes and yields electrons to Platinum and protons to the membrane:

$$H_2 \rightarrow 2H^+ + 2e^- ; \quad (1)$$

- at the cathode, the oxygen reacts with the protons coming from the membrane and with the electrons supplied by the catalyser and forms molecules of water:

$$1/2O_2 + 4H^+ + 4e^- \rightarrow 2H_2O. \quad (2)$$

The **membrane**, if well humidified, has a proton conductivity sufficiently high.
Inside the cells, however, because of the dragging of water molecules by the proton flow, the part of the membrane on the cathode side tends to saturate, while the one on the anode side tend to dehydrate, with a consequent conductivity reduction; to limit this phenomenon, and to avoid water loss by evaporation, the cell is fed with humidified gases at higher temperatures than the cell temperature.

2.2. General model description

The model considers a cell that utilises H_2 as a fuel and air as oxidant, both humidified.

The main assumptions of the proposed model are as follows:

- the model is one-dimensional, i.e., all quantities vary only in the direction orthogonal to anode and cathode surfaces;
- the temperature is supposed to be uniform in the cell;
- the air total pressure is assumed to be uniform, while the variation with space of the partial pressures of its components is kept into account;
- the water vapor contained in the reactants of the baking macropores is in equilibrium with the surrounding liquid phase; consequently the partial water pressure is uniform;

- the anodic voltage drop is disregarded with respect to the cathode ones (cf. [7,8,17]); consequently the voltage across the anode is considered to be constant.

The general arrangement of the model is as depicted in fig. 1.

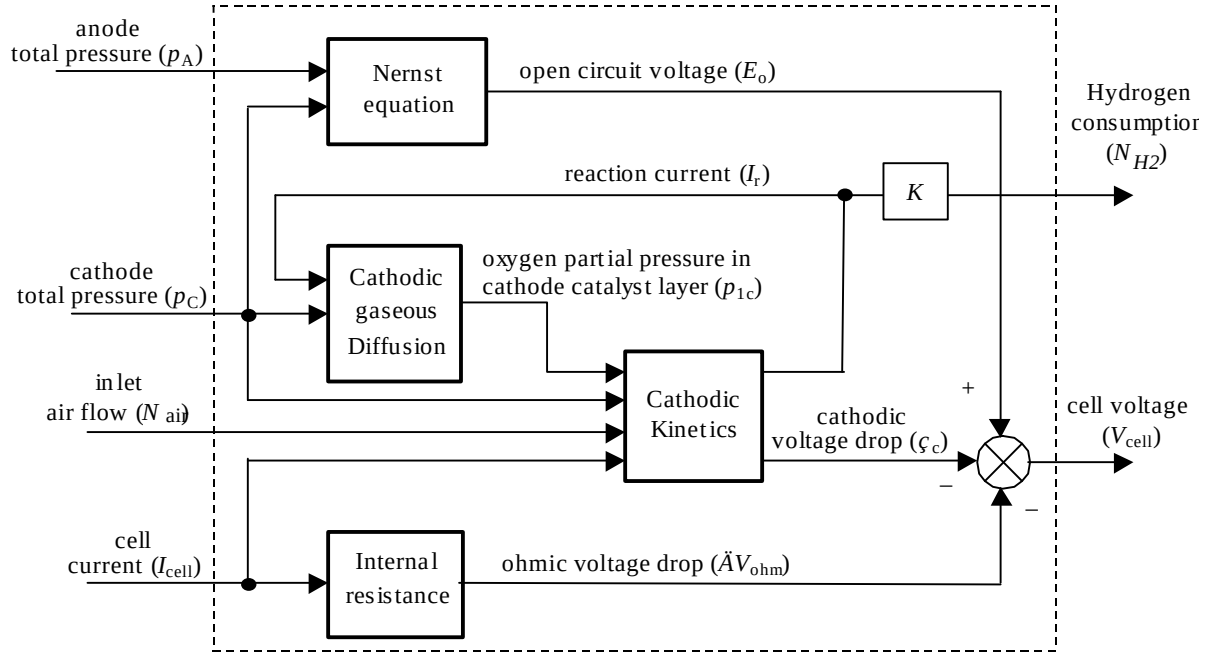

Fig. 1: Block diagram representing the general model arrangement.

As shown in the figure the model has as input the anode and cathode total pressure of reactants and water vapour, and, as electrical input the cell current I_{cell}.
The main output of the model is the cell voltage; there is also an auxiliary output constituted by the hydrogen molar consumption, that is useful for making energy balances of the cell:
input power= $N_{H2} \cdot E_{H2}$ (E_{H2} is the chemical potential energy per mole of hydrogen)
output power= $V_{cell} I_{cell}$
In the following subsections, some details on the equations defining various elements of the model are reported.

2.3. Gas Diffusion in the cathodic baking

The oxygen contained in the air entering the cell before reaching the catalyst layer diffuses, through the substrate, within a gaseous mix constituted by nitrogen, water vapour and the oxygen itself, all considered as being ideal gases. This phenomenon is described [5÷8] by the following differential equations:
continuity equations:

$$\frac{\varepsilon_g}{RT}\frac{\partial p_i}{\partial t} + \frac{\partial N_i}{\partial y} = 0 \quad ; \tag{3}$$

Stefan-Maxwell equations of diffusion:

$$\frac{\varepsilon_g}{\tau^2}\frac{\partial p_i}{\partial y} = \sum_{k=1}^{3} \frac{RT}{p D_{ik}}\left(p_i N_k - p_k N_i\right), \tag{4}$$

where $i,k \in (1,3)$ and:
p_1 = oxygen partial pressure,
$p_2 = p_{sat}(T)$ = water vapour partial pressure,
p_3 = nitrogen partial pressure,
$pD_{ik} = D_{ik} = D_{ik}(T)$.
The analytical expressions of the diffusivities $D_{ik}(T)$ have been taken from [13].

In equations (4) it has been assumed, for simplicity, that the gas motion is originated only from concentration gradients, and not from gradients of total pressure. The substrate porosity e_g (ratio between pore volume and total substrate volume) is considered independent on the cell operating conditions; the parameter t (tortuosity: ratio between actual pore length and macroscopic substrate thickness) keeps into account the fact that the distance the oxygen covers for reaching the catalytic layer is greater than the substratum thickness, because of the pore curvature.

Combining equations (3) and (4) and applying the hypotheses stated in the previous paragraph, the following single partial-differential equation can be obtained, having the unique unknown p_1 (oxygen partial pressure):

$$\frac{\partial p_1}{\partial t} = w \frac{\partial^2 p_1}{\partial x^2} - y N_{1dc} \frac{\partial p_1}{\partial x}, \qquad (5)$$

in which x is the dimensionless abscissa y / L_d, w and y are parameters depending on just cell temperature and air pressure; the variable N_{1dc} is the oxygen flow at the interface substrate-catalyst layer.
With reference to fig. 1, equation (5) constitute the block "Gas Diffusion in Cathode", that receives as input the total air pressure and the reaction current and gives as output the oxygen partial pressure in the catalyst layer.

2.4. Cathodic kinetics

The electrochemical reaction that occurs in the catalyst layer is the (2), in which the oxygen reacts with the protons present in the electrolyte and with the electrons supplied by the catalyst, thus forming water molecules.
The current that is created by the electrochemical reaction, in addition to the reactants concentration, depends on the potential difference between catalyst and electrolyte, as described by the Butler-Volmer equation [9,11]:

$$I_r = j_o A_r \left\{ \frac{p_{1c}}{p_{1o}} \frac{[\mathrm{H}^+]}{[\mathrm{H}^+]_o} \exp\left(\frac{h_C}{b} \right) - 1 \right\}, \qquad (6)$$

$$h_C = E_{oC} - \Delta f_{ce} = E_o - V_{cell} - R_i I, \qquad (7)$$

The cell current , in turn, is the sum of the reaction current plus the contribution due to the charge storage in the electrical double-layer:

$$I_{cell} = I_r + C_{dl} \frac{\partial h_C}{\partial t}; \qquad (8)$$

the double-layer capacitance C_{dl} is assumed to be constant [17].
Differently from what assumed by other papers [4, 6, 9, 11], the proton concentration $[\mathrm{H}^+]$ has been considered to be a function of the cell current. Indeed it has been considered that if the cell current, and therefore the water production (according to (2)) rises, the hydration of the polymeric electrolyte tends to rise as well, causing this way an increase in the proton concentration. This hypothesis has been introduced to correctly model the voltage overshoot visible in the cell experimental response to sudden current reductions, that was already observed in [18] without any possible explanation.
Therefore the behaviour over time of the proton concentration $[\mathrm{H}^+]$ is defined by the following differential equation:

$$u\left(-\frac{\partial c_{H^+}}{\partial t} \right) \cdot \frac{\partial c_{H^+}}{\partial t} + \frac{c_{H^+}}{t_{H^+}} = \frac{1 + a_{H^+} \cdot I_{cell}^3}{t_{H^+}}, \qquad (9)$$

in which $u(:)$ is the Heaviside function, $c_{H^+} = \frac{[\mathrm{H}^+]}{[\mathrm{H}^+]_o}$ is the dimensionless proton concentration, t_{H^+} it the time constant related to the c_{H^+} dynamics, and a_{H^+} is a parameter that links c_{H^+} to the cell current.

Studies about the cathode operation [5, 6, 11, 12] have shown that as the cell current rises the quantity of Platinum engaged in the electrochemical reaction reduces, i.e., the reaction tends to concentrate in a region of the catalyst layer smaller and smaller.
This has been attributed to the electrolyte resistivity and oxygen diffusivity, that determine voltage drop and O_2 concentration gradient respectively. To keep into account the phenomenon, that would require a large number of partial-derivatives differential equations, the parameter A_r (catalytic total surface) has been considered variable with the current:

$$A_r = A_{ro} \exp\left(-a_1 I_{cell} - a_2 I_{cell}^5\right), \tag{10}$$

and the variables that appear in eq. (6) have been considered function of only time.
Parameters a_1 e a_2 of (10) result to be function of the temperature, the partial oxygen pressure, and the air flow that feeds the cell.

From experimental measures related to the reduction of oxygen in an acid environment [1, 2] it is known that parameters b e j_o of (6) present a sudden rise for values of cathodic voltage of about 0.80 V; this phenomenon is kept into account in the model.

2.5. Internal resistance and voltage drops

The passage of current through the cell causes ohmic voltage drops basically due to the electron transfer in electrodes and in the conductive graphite plates and to the proton transfer through the membrane.
Since the conductivity of graphite is much larger than the one of the membrane [4, 12], the drops due to the electron transfer can be neglected; therefore the cell internal resistance practically coincides with that of membrane.
In general, the membrane resistance results to be a function, in addition of temperature, also of the current [15, 6], because of the dragging from anode to cathode of water molecules by the current. If the current increases, in fact, the side of the membrane on the anodic part tends to dehydrate, with a reduction of the local conductivity and an increase in the membrane resistance.
From the experimental observations made ad the ENEA's labs related to a PEM cell having a Nafion 115 membrane, the internal resistance result to be, in practice, function of only temperature (fig. 2).

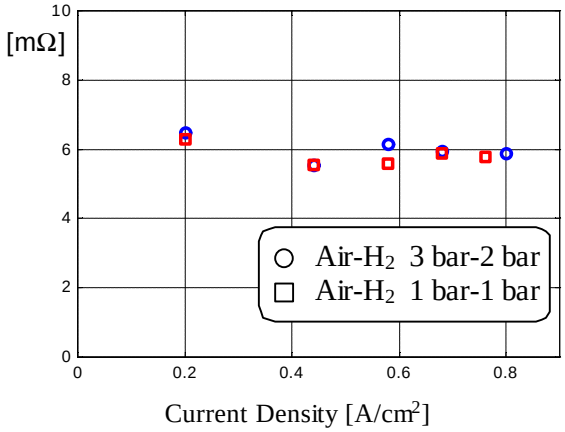

Fig. 2: Internal resistance at 70°C and different values of the reactants pressures.

Table 2: Numerical values of parameters of equation (11)

parameter	value
R_o [Ω]	5.22×10^{-3}
a_T [Ω/K]	4.24×10^{-8}
T_o [K]	338.15

Experimental data measured at different temperatures have then been interpolated by the following equation:

$$R_i = R_o + a_T \cdot (T - T_o); \tag{11}$$

The values of the parameters in (11) are reported in tab. 2, while the voltage drops related to the internal resistance are defined by the Ohm law:

$$\Delta V_{ohm} = R_i \cdot I_{cell}\,. \tag{12}$$

2.6. Open Circuit Voltage (OCV)

The open-circuit voltage has been defined by means of the Nernst equation:

$$E_o = E_{ref} + \frac{dE_o}{dT}(T - T_{ref}) + \frac{RT}{2F}\ln(p_{H_2}\, p_{O_2}^{1/2}) \qquad (13)$$

slightly modified to improve correspondence to the experimental results, as follows:

$$E_o = E_{ref} + \frac{dE_o}{dT}(T - T_{ref}) + k\,\frac{RT}{2F}\ln(p_{H_2}\, p_{O_2}^{1/2}) \qquad (14)$$

$$\mathrm{H_2(g)} + \frac{1}{2}\mathrm{O_2(g)} \rightarrow \mathrm{H_2O(aq)}\ . \qquad (15)$$

The values of parameters E_{ref} , $\frac{dE_o}{dT}$ and k (Table 3) have been determined to that to reproduce the experimental results, using the (14); in fact, with a k of 1and standard values of E_{ref} , $\frac{dE_o}{dT}$, the E_0 would be much higher than the values experimentally observed, as already noted in the past [1].
The reference temperature T_{ref} has been has been fixed to 343.15 K. In fig. 3 a comparison between measure and estimated values of E_0 is reported, with e cell temperature of 70°C and different reactant partial pressures.

Table 3: Numerical values of parameters of equation (14)

parameter	value
E_{ref} [V]	0.975
dE_o/dT [V/K]	$0.27*10^{-3}$
k	0.755

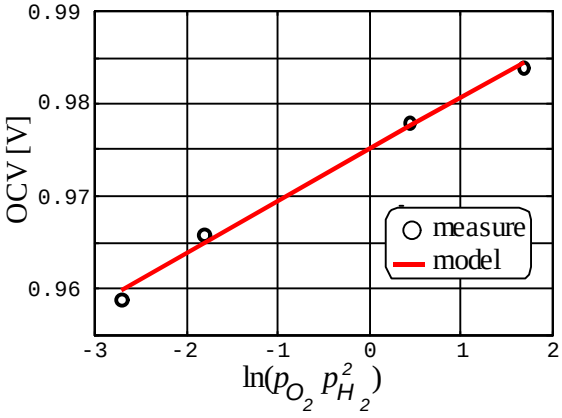

Fig. 3: Comparison of OCV measures and model for 70°C and different values of reactants partial pressures.

3. Model implementation in the Matlab/Simulink environment

For each equation that constitutes the model, it has been defined a suitable list of Matlab commands, that, in turn, are then recalled by corresponding Simulink blocks.
In particular, eq. (5), being a partial-differential equation, had been implemented using the MATLAB operator “diff”.
A vector has been built containing n discrete values of the abscissa x ($0 \le x \le 1$) and consequently the oxygen partial pressure $p_1 = p_1(x, t)$ has been considered as a vector having n components, one for each x_k of . x.
An approximation of the derivative of p_1 is given by:

$$\frac{\partial p_1}{\partial x} \cong diff\ (p_1)./\ diff\ (x)\cdot \qquad (16)$$

To find the right value of n a preliminary comparison has been made by simulating the cell in the same operating condition with several values of n; the number of n has been progressively increased up to a point in which a further increase caused negligible changes in the simulation result. In the end, a value of 100 has been assumed.

4. Comparison of simulation and experimental results

In this section a comparison between the experimental and simulated cell behaviour is reported.
The simulations have been performed using the model presented in the previous sections, filled with numerical parameters found by an identification technique that will be described in detail in a following paper.
The comparison is made both in steady state and dynamic conditions.
The cell under test, having a section of 50 cm^2, has been assembled at the ENEA's labs. The cathode has a catalyst E-TEK 20% Pt-C with 0.34 mg/cm^2 of Pt, while the anode has a catalyst realised in laboratory with 20% Pt-C and 0.29 mg/cm^2 of Pt. The membrane is a Nafion 115.
The assembly electrodes-membrane has been pressed between two graphite plates provided with serpentine channels. Reactant gases, were humidified Air and hydrogen.

In fig. 4 a comparison of steady-state experimental and simulated cell voltage under different operating conditions is reported.

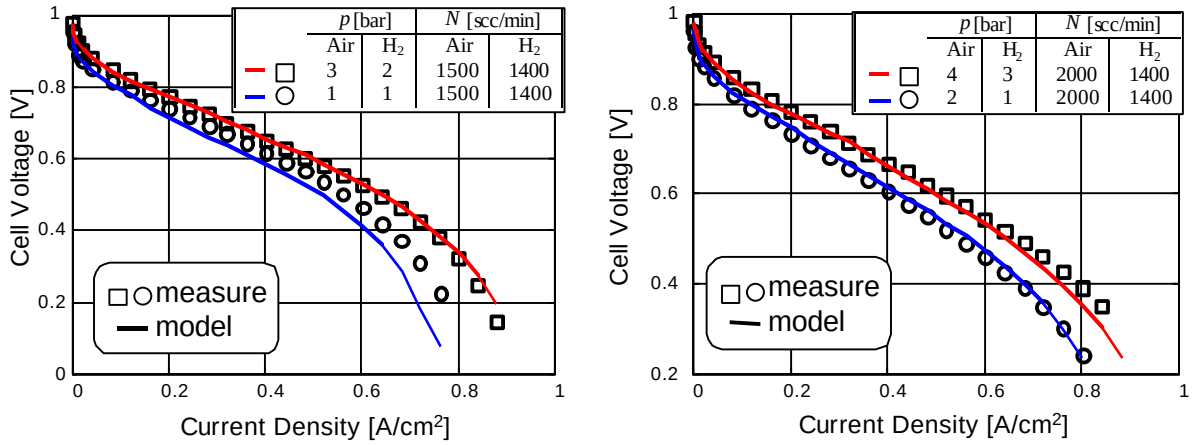

Fig. 4: Comparison of simulated and measured cell voltage at a cell temperature of 70°C and different values of reactant pressures and flows.

The figure shows a good agreement of data, especially in the region of low densities (before the knee); this region is the one having the maximum interest for practical applications; a sufficient agreement is however present also even after the curve knees.

In figures 5-6-7 the dynamic response to current steps of the model is compared with the one experimentally measured, in different cell operating conditions.
In each case a good agreement is observed on the whole transient.
In particular in the case of fig. 7, showing the response to an instantaneous interruption of the cell current, the agreement between experimental data and simulation is excellent.

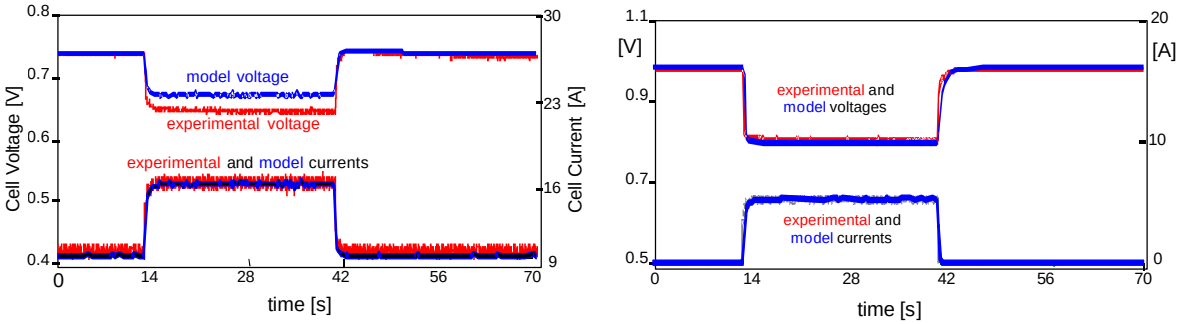

Fig. 5. Comparison of experimental and simulated cell dynamic response, considering two different current steps. Cell temp. 60°C; reactant pressures 3 bar; Air and H2 flows 1000 and 500 scc/min respect.

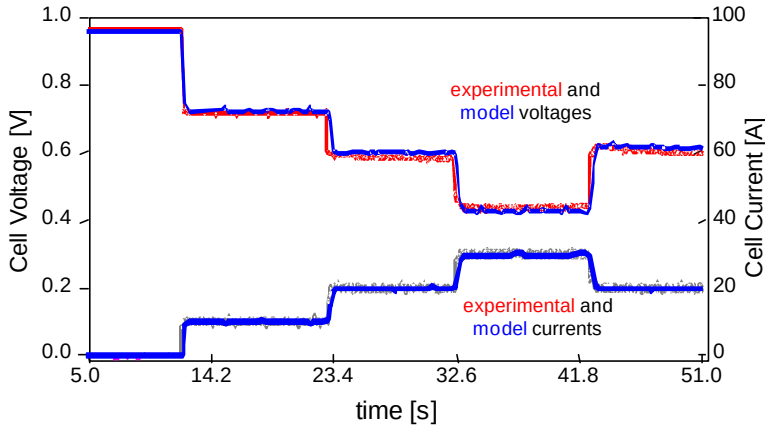

Fig. 6. Comparison of experimental and simulated cell dynamic response. Cell temp. 70°C; reactant pressures 1 bar; Air and H_2 flows 1500 and 1400 scc/min respectively.

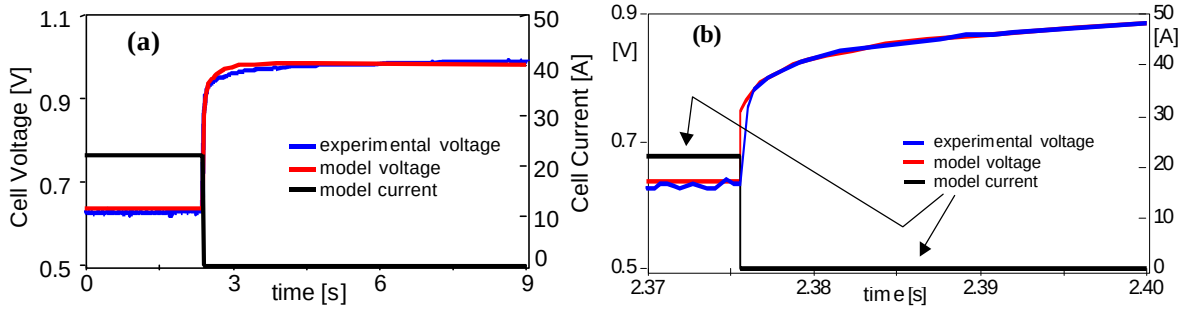

Fig. 7: Comparison of experimental and simulated cell dynamic response. Cell temp. 70°C; Air and H_2 flows pressures 3 and 2 bar; Air and H_2 flows 1500 and 1400 scc/min respectively. Fig. (b) is a zoom on a particular of figure (a).

5. Conclusions

A dynamical model of Proton Exchange Membrane fuel cell, based on physical and chemical equations, has been proposed.
This model, is noticeably simplified with respect to other chemical-physical, dynamic models already presented in literature.

The model has been implemented in the MATLAB/SIMULINK environment to test its behaviour.

The behaviour of the model has been compared with experimental tests carried out at ENEA's laboratories. This comparison shows a good agreement between measures and simulation.

This model is structured so that it can be easily extended to a whole stack of fuel cells.

6. List of symbols

A_r (effective Pt surface area): cm^2
A_{ro} (total Pt surface area): cm^2
b (Tafel slope): V
C_{dl} (double-layer capacitance): F
c_{H^+} (dimensionless proton concentration)
D_{ik} (diffusivity of the gas pair *i*-*k*): cm^2/s

D_{ik} (total pressure-diffusivity product): (atm cm^2)/s
E_o (open circuit voltage): V
E_{oC} (cathode potential): V
E_{ref} (reference voltage): V
F (Faraday's constant): 96484.56 C/equivalent
$[H^+]$ (proton concentration): mol/cm^3
I_{cell} (cell current): A
j_o (exchange current density): A/cm^2
I_r (reaction current): A
L_d (thickness of diffusion layer): cm
N_{air} (inlet air mole flow): mol/s
N_{H_2} (hydrogen consumption): mol/s
N_k (superficial flux of species k): mol/(cm^2 s)
N_{1dc} (oxygen flux at interface diffusion and catalyst layer): mol/(cm^2 s)
p_C (cathode total pressure): atm
p_k (partial pressure of species k): atm
p_{1c} (oxygen partial pressure whitin catalyst layer): atm
p_{1o} (zero-current oxygen partial pressure): atm
R (gas constant): 82.056 (atm cm^3)/(K mol) = 8.3144 J/(K mole)
R_i (internal resistance): ohm
T (absolute temperature): K
$u(:)$ (Heaviside function)
x_k (mole fraction of species k)
y (distance through diffusion layer): cm
t (tortuosity of diffusion layer)
t_{H^+} (time constant of proton concentration): s
x (dimensionless distance)
Df_{ce} (catalyst-electrolyte potential difference): V
h_C (cathode voltage drop): V
e_g (porosity in diffusion layer)

7. References

[1] A. Parthasarathy, C. R. Martin, S. Snirivasan, A. J. Appleby, *J. Electrochem. Soc*., vol. **139**, p. 2530, (1992).

[2] D. B. Sepa, M. V. Vojnovic, M. Vracar, A. Damjanovic, *Electrochimica Acta*, vol. 32, p. 129, (1987).

[3] M. Uchida, Y. Aoyama, N. Eda, A. Ohta, *J. Electrochem. Soc*., vol. **142**, p. 4143, (1995).

[4] K. Broka, P. Ekdunge, *Journal of Applied Electrochemistry*, vol. **27**, p. 281, (1997).

[5] D. M. Bernardi, M. W. Verbrugge, *AIChE Journal*, vol. 37, n. 8, p. 1151, (1991)

[6] D. M. Bernardi, M. W. Verbrugge, *J. Electrochem. Soc*., vol. **139**, p. 2477, (1992).

[7 T. E. Springer, M. S. Wilson, S. Gottesfeld, *J. Electrochem. Soc*., vol. **140**, p. 3513, (1993).

[8] T. E. Springer, T. A. Zawodzinski, S. Gottesfeld, *J. Electrochem. Soc*., vol. **138**, p. 2334, (1991).

[9] Y. W. Rho, S. Snirivasan, *J. Electrochem. Soc*., vol. **141**, p. 2089, (1994).

[10] J. C. Amphlett., R. M. Baumert, B. A. Peppley, P. R. Roberge, *J. Electrochem. Soc*., vol. **142**, p. 1, (1995).

[11] D. Bevers, M. Wohr, K. Yasuda, K. Oguro, *Journal of Applied Electrochemistry*, vol. **27**, p. 1254, (1997).

[12] C. Marr, X. Li, *Journal of Power Sources*, vol. **77**, p. 17, (1999).

[13] R. B. Bird, W. E. Stewart, E. N. Lightfoot, *Transport phenomena*, Wiley, New York, (1960).

[14] M. S. Wilson, J. A. Valerio, S. Gottesfeld, *Electrochimica Acta*, vol. 40, p. 355, (1995).

[15] T. E. Springer, T. A. Zawodzinski, J. Davey, R. Jestel, C. Lopez, J. Valerio, S. Gottesfeld, *J. Electrochem. Soc*., vol. **140**, p. 1981, (1993).

[16] T. E. Springer, T. A. Zawodzinski, M. S. Wilson, S. Gottesfeld, *J. Electrochem. Soc*., vol. **143**, p. 587, (1996).

[17] P. Bolognesi, V.Conte, G. Lo Bianco, M. Pasquali: “Hy-sim: A Modular Simulator for Hybrid-Electric Vehicles”, *The 18th International Electric Vehicle Symposium*, EVS18, October 2001, Berlin, Germany.

[18] J. C. Amphlett, E. K. De Oliveira, R. F. Mann, P. R. Roberge, A. Rodrigues, J. P, Salvador, *Journal of Power Sources*, vol. **65**, p. 173 (1997)

8. Authors

Massimo Ceraolo, Prof. Dr. Ing.
(Dipartimento di Sistemi Elettrici e Automazione, Via Diotisalvi 2, 56126 - Pisa/Italy, T: +39-50-565305, Fax: +39-50-565333, e-mail m.ceraolo@ing.unipi.it)
Got the degree in Electrical engineering at the University of Pisa in 1985.

Since 1992 he has been working at University of Pisa in Electric Power Systems first as a researcher, then as an associate professor.
Major fields of interest: Active and Reactive power compensation, Long-distance Transmission systems, Computer Simulations, Storage Batteries, Electric and Hybrid Vehicles.

Romano Giglioli, Prof. Dr. Ing.
(Dipartimento di Sistemi Elettrici e Automazione, Via Diotisalvi 2, 56126 - Pisa/Italy, T: +39-50-565338, Fax: +39-50-565333, e-mail giglioli@dsea.unipi.it)
Got the degree in Electrical engineering at the University of Pisa in 1976.

Since 1977 he has been working at University of Pisa in Electric Power Systems first as a researcher, then as an associate professor, finally as a full professor. Presently he is the dean of the Department.
Major fields of interest: Transmission systems, storage batteries, Active and Reactive power compensation, Electric and Hybrid Vehicles, Distributed Generation.

Carmine Miulli, Dr. Ing.
(Dipartimento di Sistemi Elettrici e Automazione, Via Diotisalvi 2, 56126 - Pisa/Italy, e-mail miulli@dsea.unipi.it)
Got the degree in Electrical engineering at the University of Pisa in 2000.

After having taken the degree, has worked under contract at Dipartimento di Sistemi Elettrici e Automazione of University of Pisa on the topic of Dynamic Modelling of PEM Fuel cells.
He is currently working also on Dynamic Modelling of NiMH traction batteries.

Alfonso Pozio, Dr.
(ENEA, Italian Agency for New Technology, Energy and Environment C.R Casaccia, Via Anguillarese 301, 00060 - Roma/Italy, T: +39-06-30486768, Fax: +39-06-30486357, e-mail alfonso.pozio@casaccia.enea.it
Got the degree in Chemistry at the University of Rome "La Sapienza" in 1991. Since 1992 he has been working at ENEA first under contract, then as a researcher. Major fields of interest: electrochemical characterization of components and cells, development of fabrication technologies for advanced complex membrane/electrodes (MEA), development of low Pt loading and CO tolerant electrodes, modelling of active components and cells.